Received: 4 November 2021 | Revised: 4 February 2022 | Accepted: 10 February 2022

DOI: 10.1111/jop.13321

ORIGINAL ARTICLE

Journal of Oral Pathology & Medicine WILEY

Mesenchymal stem cell-exosome-mediated matrix metalloproteinase 1 participates in oral leukoplakia and carcinogenesis by inducing angiogenesis

Shufang Li[1] | Ying Han[1] | Mingxing Lu[1] | Zijian Liu[1] | Jianqiu Jin[2] | Qianyun Guo[1] | Yixiang Wang[3] | Hongwei Liu[1]

[1]Department of Oral Medicine, Peking University School and Hospital of Stomatology, Beijing, China

[2]Department of Stomatology, Beijing Hospital, National Center of Gerontology, Beijing, China

[3]Department of Central Laboratory, Peking University School and Hospital of Stomatology, Beijing, China

Correspondence
Yixiang Wang, Department of Central Laboratory, Peking University School and Hospital of Stomatology, No 22 Zhongguancun Ave South, Haidian District, Beijing 100081, China.
Email: kqwangyx@bjmu.edu.cn

Hongwei Liu, Department of Oral Medicine, Peking University School and Hospital of Stomatology, No 22 Zhongguancun Ave South, Haidian District, Beijing 100081, China.
Email: hongwe1l2569@163.com

Funding information
National Natural Science Foundation of China (Grant Nos 81771071, 81977920, 81772873)

Abstract

Background: In the malignant progression of oral leukoplakia (OLK) to oral squamous cell carcinoma (OSCC), the density of microvessels and expression of angiogenesis-related molecules increases. Emerging evidence indicates that mesenchymal stem cells (MSCs) play an indispensable role in the tumor microenvironment. However, the role and mechanism of action of oral MSCs in inducing angiogenesis remain unclear. Therefore, it is necessary to explore the molecules and mechanisms that play a role in the tissue microenvironment.

Methods: Exosomes were collected from normal oral mucosa (N-Exo), OLK (OLK-Exo), and OSCC (Ca-Exo) MSCs, and their pro-angiogenic capacity was evaluated in human umbilical vein endothelial cells (HUVECs) and a subcutaneously implanted tumor model in nude mice. Quantitative proteomics analysis was used to compare the exosome-derived proteins between N-Exo, OLK-Exo, and Ca-Exo.

Results: Compared with that of the N-Exo and control, OLK-Exo and Ca-Exo treatment significantly promoted HUVEC migration, invasion, and tube-formation capability. In the nude mice model, immunofluorescence of CD31 showed that OLK-Exo and Ca-Exo substantially improved neovascularization around the grafts. Quantitative proteomics analysis revealed that matrix metalloproteinase 1 (MMP1) levels were significantly higher in the OLK-Exo and Ca-Exo groups than in the N-Exo groups. Silencing MMP1 expression reversed the functional promoting effect of OLK-Exo and Ca-Exo on HUVECs.

Conclusion: Exosomes from OLK-MSCs and Ca-MSCs have a stronger pro-angiogenic ability through high MMP1 content. This new finding provides insight into the intervention with the secretion of MSC-derived exosomes, which may be an innovative strategy for carcinogenesis.

KEYWORDS
angiogenesis, exosome, mesenchymal stem cells (MSCs), oral leukoplakia (OLK), oral squamous cell cancer (OSCC)

1 | INTRODUCTION

Oral squamous cell carcinoma (OSCC) is the most common oral tumor and is a serious public health problem.[1,2] Despite certain advances in treatments such as surgery, chemotherapy, and radiotherapy, the 5-year survival rate remains low.[3] OSCC generally precedes oral potentially malignant disorders, with special emphasis on oral leukoplakia (OLK).[4] Ideally, interception and

management of OSCC at an early stage may improve the patients' prognosis and quality of life.[5] To date, the pathogenesis and carcinogenesis of OLK have not been fully elucidated. There is an urgent requirement to explore the potential mechanisms of action to prevent OLK and OSCC and improve therapeutic approaches.

Malignant transformation includes internal dysregulation of cancer cells and the influence of the complex tumor microenvironment (TME).[6] The TME influences cell fate in various ways, such as cancer cell proliferation and differentiation, promoting angiogenesis, invasion, and metastasis.[6] Angiogenesis is the basic feature of tumor cells. Microvessel density may be a prognostic factor for several malignant lesions, including OSCC.[7] Pazouki reported an increase in microvascular volume from normal oral mucosa to mild, moderate, and severe dysplasia, and to early and late OSCC.[8] However, the underlying mechanism of how angiogenesis affects OLK and carcinogenesis is predominantly unknown. Therefore, it is necessary to explore the molecular mechanism of angiogenesis-related malignant transformation from OLK to OSCC.

Mesenchymal stem cells (MSCs) have generated considerable interest, as they are recruited into the TME and favor tumor progression. MSCs recruited to the TME have a unique expression profile and proto-oncogenic function, and are considered to be a subset of cells with the highest tumorigenic ability and are associated with tumor recurrence. MSCs modulate the TME via autocrine and paracrine production of promotive factors related to tumor cell proliferation, angiogenesis, invasion, inflammation, and metastasis.[9–11] Exosomes, as the main paracrine products of MSCs, can maintain structural stability and prevent the degradation of contents.[12] Exosomes play an important role in the microenvironment of OLK malignant transformation and OSCC metastasis.[13,14] However, whether MSC-derived exosomes affect oral mucosal angiogenesis, and the mechanism of this effect is not fully elucidated.

Due to the complexity of OLK and OSCC, the roles of MSCs and exosomes residing in their microenvironment are undetermined. In this study, we investigated the effect of N-Exo (mucocele-derived exosomes), OLK-Exo (OLK-derived exosomes), and Ca-Exo (OSCC-derived exosomes) on vascular endothelial cells, explored the malignant transformation mechanism of OLK, and provided strategies for the prevention and treatment of OLK and OSCC.

2 | MATERIALS AND METHODS

2.1 | Collection of biological material

Oral mucosal tissue was collected from patients requiring histopathological biopsy, including mucocele, OLK, and OSCC, at the Peking University School of Stomatology. Samples were stored in MSC medium (ScienCell) with 4% penicillin/streptomycin (P/S, ScienCell). This study was approved by the ethics committee of the Peking University School of Stomatology.

2.2 | Generation and identification of MSCs from oral lesions

N-MSCs (mucocele-derived MSCs), OLK-MSCs (OLK-derived MSCs), and Ca-MSCs (OSCC-derived MSCs) were isolated and identified as previously reported.[15] Briefly, primary MSCs were isolated from tissue blocks and collected as a third generation for further study. MSCs were stained with DIO and DAPI, and observed under a fluorescence microscope. Alizarin Red and Oil Red O stainings were used for osteogenic and adipogenic differentiation. Flow cytometry was used to detect MSC-related surface markers (CD29, CD31, CD45, and CD73; BioLegend). Human umbilical vein endothelial cells (HUVECs) were acquired from the Department of Central Laboratory at the Hospital of Stomatology and cultured in M199 medium (ScienCell) supplemented with 10% fetal bovine serum (ScienCell) and 1% P/S.

2.3 | Isolation and identification of exosomes

The culture medium of N-MSCs, OLK-MSCs, and Ca-MSCs was obtained and centrifuged at 300*g* for 10 min, 2000*g* for 20 min, and 10 000*g* for 30 min. The supernatant was then centrifuged at 100000*g* for 70 min at 4°C. Finally, the pellets were suspended in phosphate-buffered saline (PBS). The total protein concentration was quantified using a BCA assay kit (Solarbio). To identify the features of exosomes, their morphology was observed using transmission electron microscopy (TEM). Nanoparticle tracking analysis (NTA) was performed to determine the size distribution and concentration. The specific surface markers (CD9, CD63, CD81, Hsp70, TSG101, and calnexin) were detected by western blotting.

2.4 | Internalization of exosomes

Exosomes were labeled with the red fluorescent dye PKH26 (Sigma-Aldrich). HUVECs were cultured with PKH26-labeled exosomes for 6 h followed by 4% paraformaldehyde fixation, and the nuclei were stained with DAPI. HUVECs were then observed using a laser confocal microscope (Leica).

2.5 | Cell proliferation assay

Cell proliferation was evaluated using the Cell Counting Kit-8 (CCK-8) assay. HUVECs were seeded onto 96-well plates at a density of 2×10^3 cells/well and treated with PBS, N-Exo, OLK-Exo, or Ca-Exo (100 μg/ml) for 24, 48, and 72 h. CCK-8 (10 μl per well) was added to the culture medium at 37°C for 2 h. The absorbance was read by microplate spectrophotometer (Bio-Rad) at 450 nm.

2.6 | Cell migration assay

A wound-healing assay was performed to assess HUVEC migration in vitro. HUVECs were treated with PBS, N-Exo, OLK-Exo, or Ca-Exo (100 μg/ml) for 24 h. Next, HUVECs were harvested and seeded in a six-well plate at a density of 1×10^5 cells/well. The next day, the confluent monolayer was scratched with a 200-μl pipette tip scratch, and the floating cells were washed with PBS. The wound was photographed at 0 and 24 h after scratching. Cells were imaged under a phase-contrast microscope, and the migrated cells were calculated and plotted using ImageJ software.

2.7 | Cell invasion assay

HUVEC invasion was tested in a Transwell Boyden Chamber (8 μm), with membrane inserts coated with diluted Matrigel (Corning). HUVECs were seeded in the upper chamber with 0.2 ml stimulant (100 μg/ml of N-Exo, OLK-Exo, and Ca-Exo). The lower chamber was filled with 0.8 ml serum-free medium. After incubation for 24 h, the cells were fixed and stained with 0.1% crystal violet, and the upper cells were wiped off using a cotton swab. Images were captured using a photo-microscope and quantified by counting at least three fields.

2.8 | Tube formation assay

HUVECs were treated with exosomes (100 μg/ml of N-Exo, OLK-Exo, or Ca-Exo) for 24 h and then harvested. Matrigel was added to a pre-chilled 96-well plate and solidified at 37°C for 0.5 h. Pretreated HUVECs (2×10^4 cells/well) were added to each well. The cells were treated for 6 h at 37°C, and the structures of the formed tubes were observed using an inverted microscope.

2.9 | Isolation of cellular and exosomal proteins and western blotting

RIPA buffer (Beyotime) was used to extract proteins from cells and exosomes. Total protein was quantified using a BCA kit and subjected to 10% SDS-PAGE gel. The gel was transferred onto PVDF membranes and blocked with 5% bovine serum albumin, followed by incubation with primary antibodies at 4°C overnight. The bands were then incubated with secondary antibodies for 1 h and visualized using an ECL plus system (Solarbio). The following primary antibodies were used: CD9 (ab263019, Abcam), CD63 (ab134045, Abcam), CD81 (ab109201, Abcam), Hsp70 (ab181606, Abcam), TSG101 (ab125011, Abcam), Calnexin (ab133615, Abcam), VEGFR2 (ab134191, Abcam), VEGFA (ab214424, Abcam), CD31 (02638, ImmunoWay), MMP1 (ab134184, Abcam), and β-actin (Proteintech). Quantitative densitometric analysis of the bands was performed using the ImageJ software. β-actin and CD9 were used as internal references for cells and exosomes, respectively, and the ratio of the gray value of the electrophoresis band to β-actin and CD9 were used as internal controls. The experiment was repeated three times, and the average value was used for relative quantitative analysis.

2.10 | In vivo Matrigel plug assay in mice

Female BALB/c nude mice (6 weeks old) were obtained from Vital River Laboratories. All experimental procedures were approved by the Animal Ethics Committee of Peking University Health Science Center. The mice ($n = 8$) were injected with 300 μl Matrigel (Corning) + Cal27 cells (2×10^4) into the subcutaneous tissue of the right axilla. After 2 weeks, the mice were randomly divided into four groups, and each group was injected with PBS, N-Exo, OLK-Exo, or Ca-Exo (100 μg/each site) into the Matrigel once weekly for 2 consecutive weeks. Fourteen days after exosome injection, the mice were sacrificed, and the grafted samples were collected for histological examination.

2.11 | Histological examination

To quantitatively determine the vessels in the Matrigel plugs, hematoxylin and eosin (H&E) and immunohistochemistry (IHC) for CD31 were performed. Matrigel plugs were fixed in 10% neutral buffered formalin, embedded in paraffin, and sectioned at 5 μm. After dehydration and antigen repair, 5-μm-thick sections were incubated with the CD31 primary antibody (ab28364, Abcam) before treatment with a secondary antibody. Finally, the samples were colored using a DAB substrate.

2.12 | Tryptic digestion and tandem mass spectrometry (MS/MS) analysis

Fresh N-Exo, OLK-Exo, and Ca-Exo were lysed for MS/MS analysis. First, protein concentration was measured using a BCA kit. After trypsin digestion, the peptides were desalted using Strata X C18 and vacuum freeze-dried. The tryptic peptides were fractionated by high-pH reverse-phase high-performance liquid chromatography, dissolved in 0.1% formic acid, and loaded onto an EASY-NLC 1000 Ultra-Performance Liquid Chromatography (UPLC) system. The peptides were treated with a nano spray ionization source followed by MS/MS in a Q Exactive TM Plus (Thermo Fisher Scientific) coupled online to the UPLC system. MS RAW data files were uploaded to Mascot 2.1 via Proteome Discoverer.

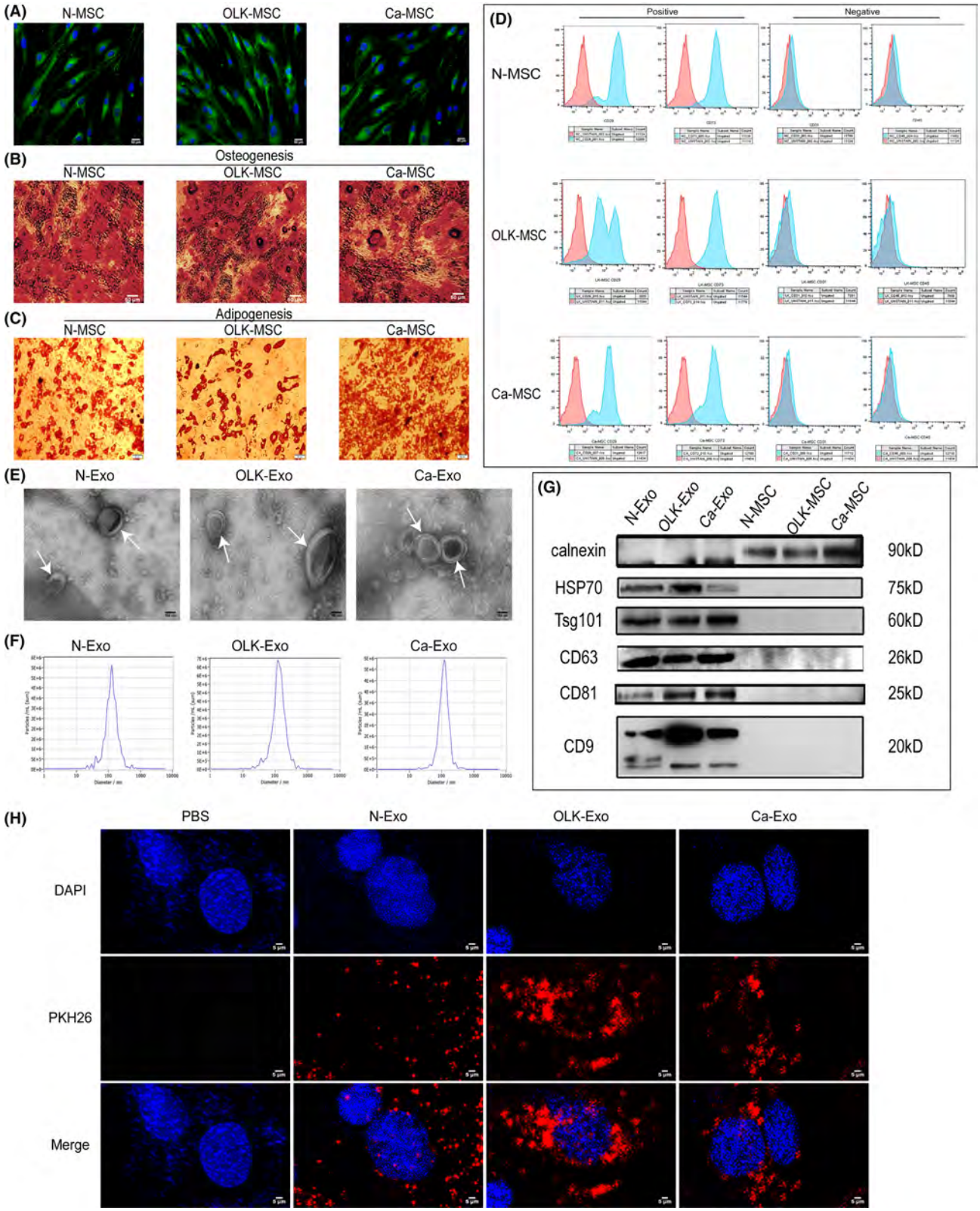

FIGURE 1 Identification of N-MSCs, OLK-MSCs, Ca-MSCs, N-Exo, OLK-Exo and Ca-Exo. (A) Morphology of N-MSC, OLK-MSC, and Ca-MSC. (B) MSCs cultured in osteogenic inductive conditions for 21 days, mineralized nodules found by Alizarin Red staining. (C) Cultured MSCs formed Oil Red O-positive lipid cluster following 21 days of adipogenic induction. (D) Flow cytometric analysis of ex vivo expanded MSCs revealed positive expression of CD29, CD73, and negative expression of CD31, and CD45. (E) Morphology of N-Exo, OLK-Exo, and Ca-Exo visualized by TEM. (F) The size distribution of N-Exo, OLK-Exo, and Ca-Exo was detected via NTA. (G) The specific surface markers (CD9, CD63, CD81, Hsp70, and TSG101) of exosomes were assessed by Western blotting. (H) The internalization of exosomes by HUVECs via laser scanning confocal microscopy. Exosomes and cell nucleus were stained red and blue, respectively. MSC, mesenchymal stem cell; NTA, nanoparticle tracking analysis; TEM, transmission electron microscopy.

2.13 | Statistical analysis

All experiments were performed in triplicate. Statistical analyses were conducted using GraphPad Prism software (version 8.0). The differences between the two groups were analyzed using an unpaired Student's *t*-test. Differences between >3 groups were analyzed using one-way ANOVA. Data are presented as the mean ± standard deviation (SD). Statistical significance was set at $p < 0.05$.

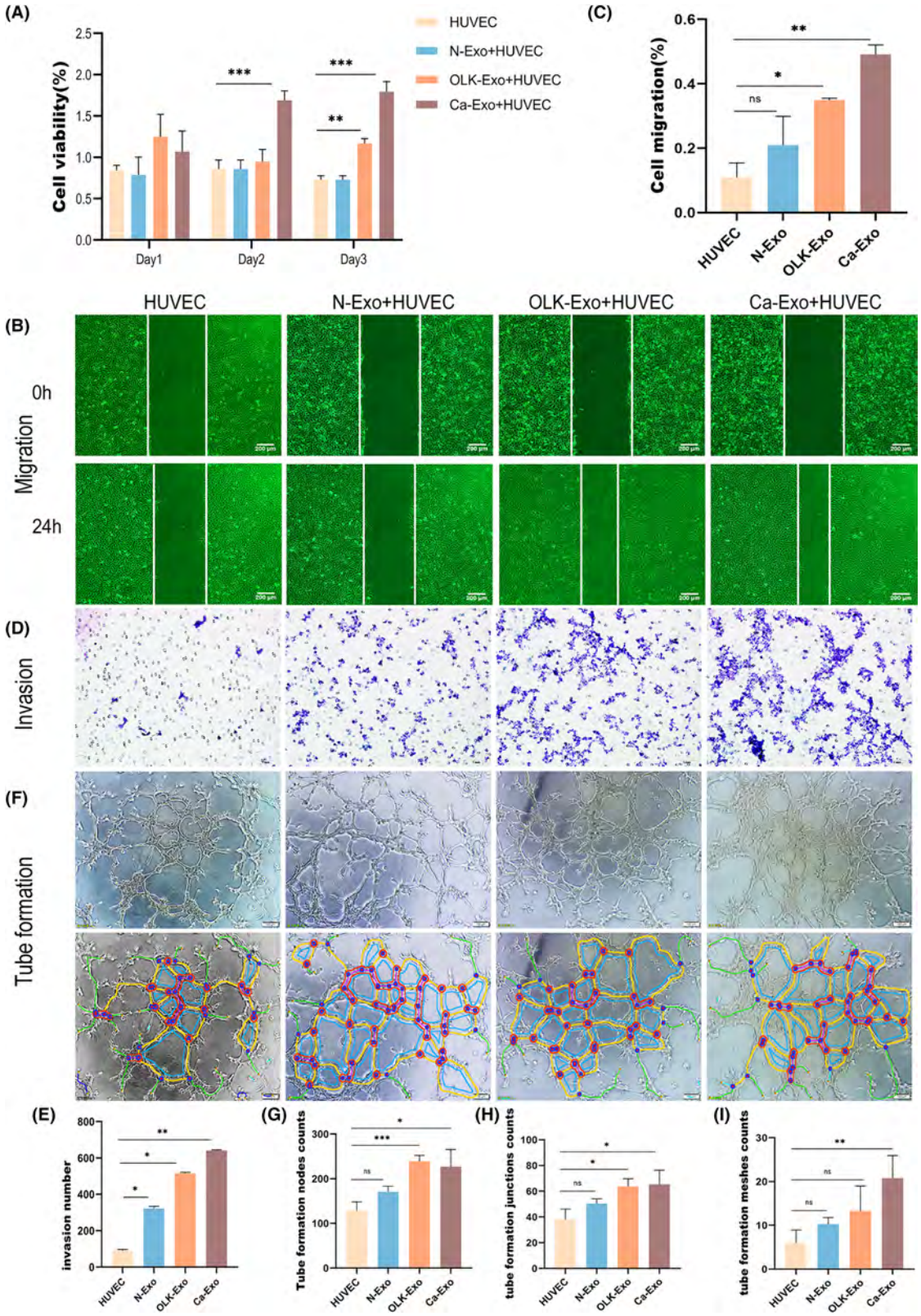

FIGURE 2 Legend on next page.

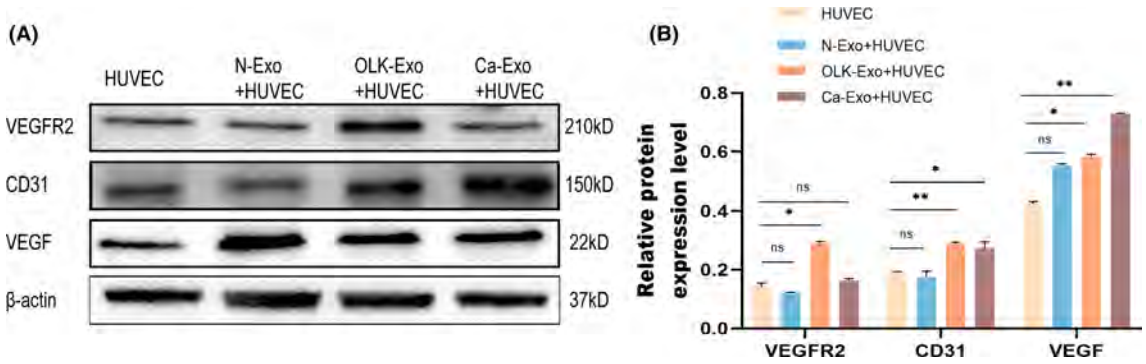

FIGURE 3 (A, B) Western blot data suggested the protein expressions of vascular endothelial growth factor, vascular endothelial growth factor receptor 2, and endothelial cell adhesion molecule-1 (CD31) were elevated in the OLK-Exo and Ca-Exo groups than in the N-Exo and control groups. The cropped bands represent independent experiments in duplicate for each protein; β-actin was used as the internal control. Data are expressed as proteins/β-actin ratio ± SD. Data are mean ± SD. $n = 3$ in each group. $^{*}p < 0.05$; $^{**}p < 0.01$ by Student's t-test, ns: no significance. HUVEC, human umbilical vein endothelial cell.

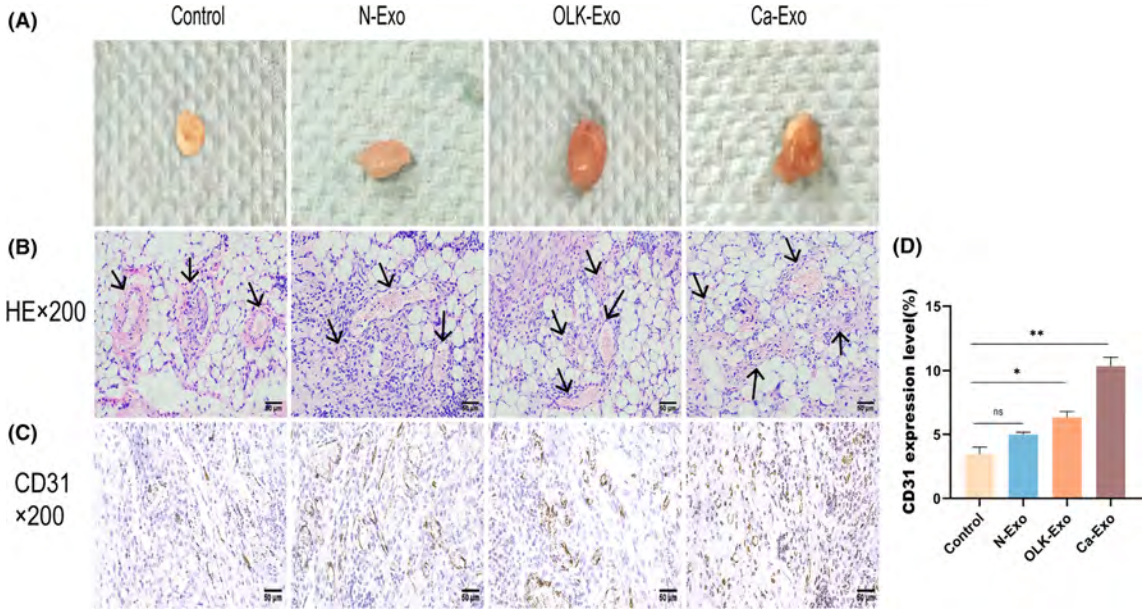

FIGURE 4 Treatment with N-Exo, OLK-Exo, and Ca-Exo increased the number of blood vessels in a Matrigel plug mouse model. (A) Images showed that more neovascularization under Ca-Exo condition, and the fewest blood vessels in the control group. (B) Representative photograph of H&E staining of the Matrigel plugs for the control and Matrigel + N-Exo, OLK-Exo, and Ca-Exo (100 μg) groups; black arrows denote blood vessels, scale bar = 50 μm. (C, D) The neovessels induced by the exosomes in Matrigel were visualized by immunohistochemical staining with CD31 antibody, scale bar = 50 μm. Data are mean ± SD. $n = 3$ in each group. $^{*}p < 0.05$; $^{**}p < 0.01$ by Student's t-test, ns: no significance. H&E, hematoxylin and eosin.

FIGURE 2 Exosomes derived from N-MSCs, OLK-MSCs, and Ca-MSCs induce angiogenesis in HUVECs. (A) Graph showing the proliferation of HUVECs quantified via CCK8 assay after 24, 48, and 72 h treatment with 100 μg/ml of N-Exo, OLK-Exo, and Ca-Exo. (B) An artificial wound was created on the monolayer of HUVECs at time zero. After capturing the denuded area in each well, cells were incubated with indicated concentrations of exosomes for 24 h; the denuded area was then captured at 24 h (C) and the percentages of wound recovery were calculated. (D) OLK-Exo and Ca-Exo promoted invasion of HUVECs. HUVECs were plated in the upper chamber and then incubated with exosomes (100 μg/ml) for 24 h. Photomicrographs depict the migrated HUVECs at the end of the experiment. (E) The number of invasive was counted, and the results were presented as mean ± SD, from three individual experiments. (F) Endothelial tube formation of HUVECs cultured with PBS, N-Exo, OLK-Exo, and Ca-Exo for 6 h. ImageJ software was used to analyze the images, and the vessels (red lines) and junctions (blue dots) are shown. (G–I) The relative number of nodes, junctions, and meshes were measured in the images using ImageJ software. Data are mean ± SD. $n = 3$ in each group. $^{*}p < 0.05$; $^{**}p < 0.01$; $^{***}p < 0.001$ by Student's t-test. ns = no significance. HUVEC, human umbilical vein endothelial cell; MSC, mesenchymal stem cell; PBS, phosphate-buffered saline.

3 | RESULTS

3.1 | Identification of MSCs and MSC-Exo

After primary MSC tissue isolation and inoculation, N-MSCs, OLK-MSCs, and Ca-MSCs derived from the oral mucosal tissue grew into a spindle shape (Figure 1A). Cytochemical staining showed the differentiation potential of N-MSCs, OLK-MSCs, and Ca-MSCs for osteogenesis and lipid formation after osteogenic and adipogenic induction, respectively (Figure 1B,C). The immunophenotypes of MSCs were characterized using flow cytometry. The results showed high expression of CD29 and CD73, and low expression of CD31 and CD45 (Figure 1D).

Subsequently, N-Exo, OLK-Exo, and Ca-Exo were identified using TEM, which showed that the three exosome types had a classic cup shape with a diameter of approximately 100 nm (Figure 1E). The exosome size distribution was assessed using the NTA. As shown in Figure 1F, the mode curve is linear and smooth, indicating few impurities, and the peak size of 125 nm is consistent with the theoretical size. The surface marker proteins were detected by western blotting, which showed that exosomes were positive for CD9, CD63, CD81, Hsp70, and TSG101, and negative for calnexin (Figure 1G). Additionally, PKH26 was used to label exosomes to detect internalization (Figure 1H), and red fluorescent protein-labeled exosomes were generally distributed around the cell nucleus. These results confirmed that

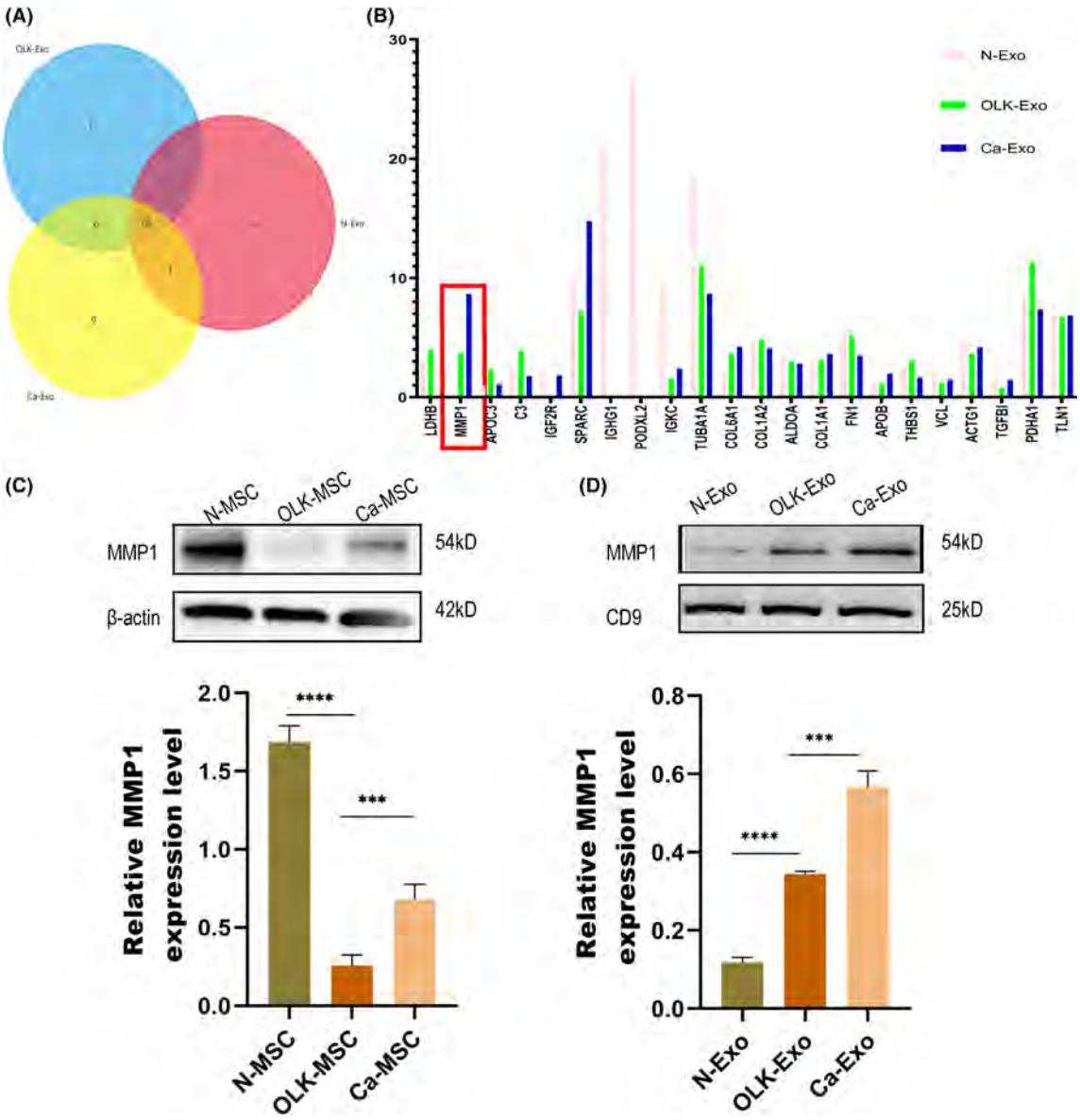

FIGURE 5 Proteomic analysis results. (A) A total of 195 proteins were identified from three groups. Twenty-two proteins with significantly different expression levels were identified by quantitative proteomic tandem mass label analysis of N-Exo, OLK-Exo, and Ca-Exo. (B) The expression level of MMP1 is the most different among N-Exo, OLK-Exo, and Ca-Exo. (C) Western blot analysis revealed the difference of MMP1 expression between N-MSCs, OLK-MSCs, and Ca-MSCs. (D) Western blot analysis of exosome proteins showed that MMP1 levels in OLK-Exo and Ca-Exo were significantly higher than those in N-Exo. *$p < 0.05$; **$p < 0.01$; ***$p < 0.001$ by Student's t-test, ns: no significance. MMP1, matrix metalloproteinase 1; MSC, mesenchymal stem cell.

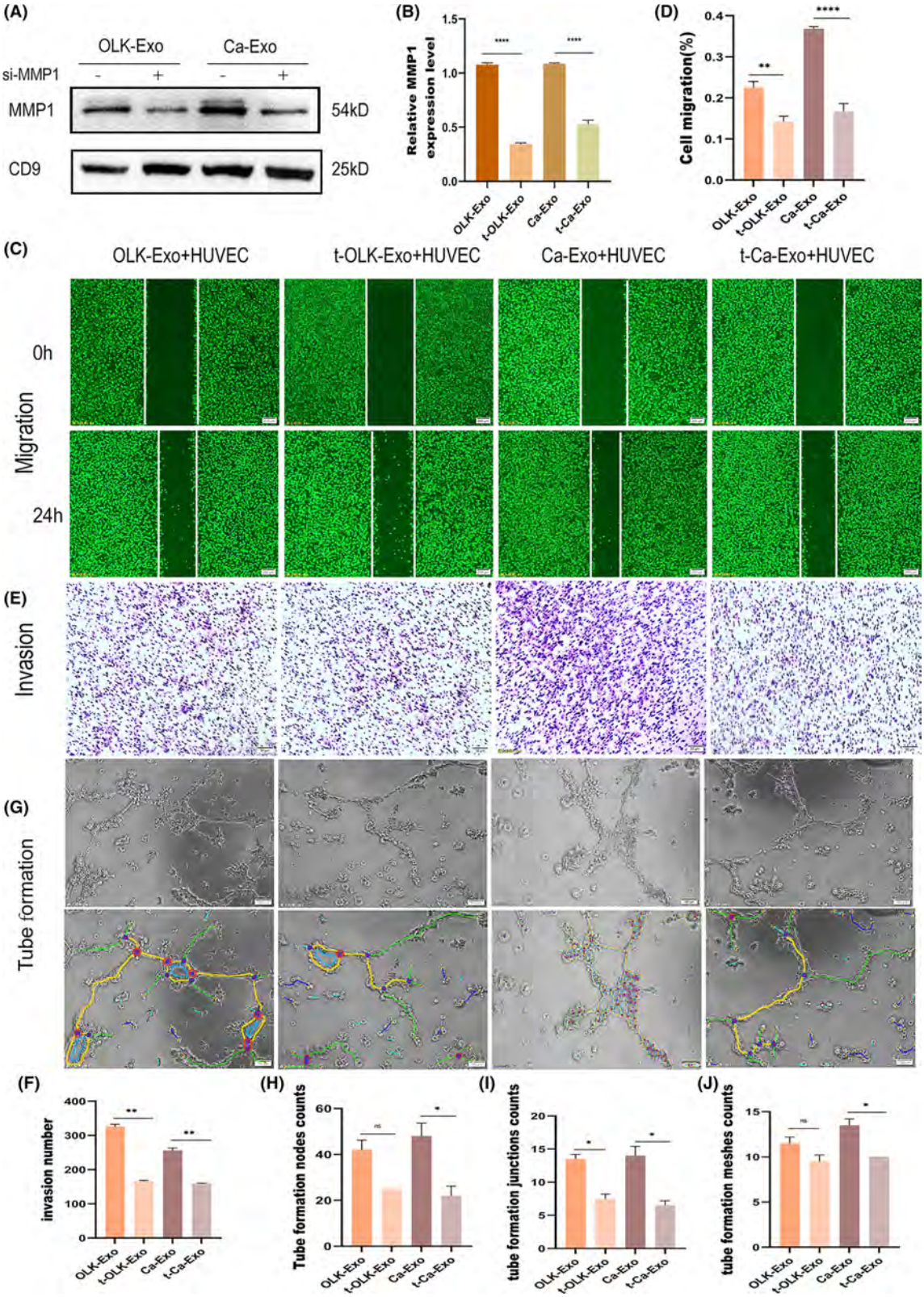

FIGURE 6 Knockdown of MMP1 attenuated the angiogenesis that was induced by OLK-Exo and Ca-Exo. (A, B) The expression level of MMP1 in OLK-Exo and Ca-Exo with or without si-MMP1. The results revealed that silencing of MMP1 reduced the enhanced migration of HUVECs that was induced by the OLK-Exo and Ca-Exo (C, D), as well as the enhanced HUVECs invasion (E, F), and tube formation (G–I). Data are mean ± SD. $n = 3$ in each group. $^{*}p < 0.05$; $^{**}p < 0.01$; $^{***}p < 0.001$ by Student's t-test, ns: no significance. HUVEC, human umbilical vein endothelial cell; MMP1, matrix metalloproteinase 1.

N-Exo, OLK-Exo, and Ca-Exo were intact, without cellular contamination, and could also be endocytosed by HUVECs.

3.2 | OLK-Exo and Ca-Exo promote biological functions of HUVECs in vitro

CCK-8 results showed that Ca-Exo significantly promoted HUVEC proliferation (Figure 2A). Scratch test results revealed that OLK-Exo and Ca-Exo significantly enhanced HUVEC migration compared with that of the N-Exo and control (PBS-treated HUVECs) groups (Figure 2B,C). The Transwell invasion assay confirmed that N-Exo, OLK-Exo, and Ca-Exo enhanced HUVEC invasion after treatment for 24 h, and Ca-Exo had the strongest effect (Figure 2D,E). Microscopic observation and quantitative analysis of microtube formation test showed that OLK-Exo and Ca-Exo promoted tubular formation of HUVECs at 6 h compared with that of the N-Exo and control groups (Figure 2F–I). Taken together, these experiments demonstrated that OLK-Exo and Ca-Exo significantly enhanced HUVEC angiogenesis.

3.3 | OLK-Exo and Ca-Exo promote the CD31/VEGF level of HUVECs

Western blotting showed that the protein expression of vascular endothelial growth factor (VEGF), vascular endothelial growth factor receptor 2 (VEGFR2), and endothelial cell adhesion molecule-1 (CD31) were elevated in the OLK-Exo and Ca-Exo groups (Figure 3A,B).

3.4 | OLK-Exo and Ca-Exo promote angiogenesis in vivo

To analyze the angiogenic response to N-Exo, OLK-Exo, and Ca-Exo in vivo, a Matrigel plug angiogenesis assay was performed in the transplanted gel plugs in nude mice. The images showed that exosomes induced more neovascularization under the Ca-Exo condition, and the fewest blood vessels were observed in the control (Figure 4A). Cross sections of the plugs were stained with H&E, confirming the presence of blood vessels in all groups (Figure 4B). The neovessel line density in the Matrigel plugs was identified by IHC using CD31. The plugs containing OLK-Exo and Ca-Exo significantly increased the density of CD31+ neovessels compared to that of the N-Exo and control groups (Figure 4C,D). These results confirmed that OLK-Exo and Ca-Exo are capable of pro-angiogenesis in vivo.

3.5 | Quantitative proteomics analysis identifies MMP1 as a key target protein

To determine the difference between N-Exo, OLK-Exo, and Ca-Exo, a quantitative proteomics analysis was conducted. A total of 195 proteins were identified, including 22 quantified proteins. The Venn diagram in Figure 5A shows 18 co-expressed proteins. A summary of all the differentially expressed proteins identified in this study is shown in Figure 5B. The expression level of MMP1 is the most different among the three exosome types, and MMP1 can promote the angiogenic activity of endothelial cell angiogenisis[16]; therefore, exosomal MMP1 was the focus for further investigation. MMP1 was determined to be highly expressed in OLK-Exo and Ca-Exo, however, it was almost undetectable in N-Exo (Figure 5D), and the MMP1 content in the cells did not conform to this expression pattern (Figure 5C). These results indicate that MMP1 in exosomes, but not in cells, may play an essential role in stimulating angiogenesis.

3.6 | Knockdown of MMP1 reduces OLK-Exo and Ca-Exo functional effects in HUVECs

To investigate whether HUVECs were affected by exosomal MMP1, siRNA was used to knock down MMP1 levels in OLK-MSCs and Ca-MSCs. We re-collected supernatant, extracted exosomes from siMMP1 transfected OLK-MSCs and Ca-MSCs, named (t-OLK-Exo and t-Ca-Exo, t = transfection), and conducted angiogenic experiments. Western blotting showed that MMP1 expression decreased in t-OLK-Exo and t-Ca-Exo cells (Figure 6A,B). The angiogenic experiment results revealed that MMP1 knockdown reduced the enhanced migration (Figure 6C,D), invasion (Figure 6E,F), and tube formation (Figure 6G–I) of HUVECs induced by OLK-Exo and Ca-Exo. Taken together, these results suggest that MMP1-enriched exosomes derived from OLK-MSCs and Ca-MSCs enhanced HUVEC angiogenesis, and that silencing MMP1 partially reversed these effects.

4 | DISCUSSION

MSCs can enhance the functional activity of OLK and OSCC through exosome miR-8485.[17] We continued to study the function of MSC-Exo in endothelial cells. Studies have revealed that exosomes mediate the biological behavior of tumor cells by delivering non-coding RNA.[18] Few studies have evaluated the function of exosomal proteins, particularly in tumor angiogenesis. The present study revealed that OLK-Exo and Ca-Exo enhanced angiogenic activity in vivo and in vitro. This result supports the phenomenon of increased microvessel density in OLK and OSCC.[19]

MMPs are a family of zinc-dependent endopeptidases that are overexpressed in several malignant tumors. Among them, MMP1 is known as collagenase and degrades collagen type I and III by recognizing the substrate through a hemopexin-like domain.[20] MMP1 is highly expressed in driving tumor progression in aggressive lung cancer[21] and contributes to hepatocellular carcinoma cell migration and invasion.[22] MMP1 expression is upregulated in oral lichen planus, dysplasia, squamous cell carcinoma, and lymph node metastasis.[23] Elevated MMP1 protein expression is associated with a higher histopathological grade of OSCC.[24] S100A14 regulates the invasive potential of OSCC-derived cell lines in vitro by modulating MMP1 expression.[25] MMP1 can induce HUVEC growth and subsequent sprouting

angiogenesis in vivo and in vitro. These studies focused on the expression and effects of MMP1 in OSCC tissues and cells, consistent with our results, while the role and mechanism of MMP1 in OLK and OSCC MSC exosomes have not been investigated. Our results revealed that MMP1 was significantly upregulated in OLK-Exo and Ca-Exo, indicating that MMP1 may promote the enhanced functional activity of HUVECs. In addition to MMP1, there were differences in protein expression levels of N-Exo, OLK-Exo, and OSCC-Exo. For instance, studies have reported that APOB does not change significantly in the peripheral blood of patients with acute spinal cord injury, however, APOB expression in peripheral plasma exosomes increases significantly. These results suggest that plasma exosomes are involved in the regulation of lipid metabolism in the acute stage of spinal cord injury, and may be involved in the regulation of metabolic reprogramming of tissue microenvironments in other diseases.[26]

In our study, we knocked down MMP1 in OLK-MSCs and Ca-MSCs using siRNA, and might have changed the other content of exosomes; more convincing evidence should be provided by either direct knockout exclusion of MMP1 or via MMP1-specific immune neutralization in exosomes. Future studies should focus on identifying the key downstream molecules and pathways to better understand the significance of exosomal MMP1 in preparing the precancerous and premetastatic niche. Our in vitro and in vivo models may not directly reflect the microenvironment of OLK and OSCC in patients; therefore, further exploration is required in the future.

5 | CONCLUSION

Taken together, our data suggest that OLK-MSC- and Ca-MSC-derived exosomal MMP1 promote HUVEC migration and angiogenesis. These findings suggest that MMP1 may be a potential therapeutic target for the clinical treatment of OLK and OSCC.

AUTHOR CONTRIBUTIONS

Hongwei Liu, Yixiang Wang, and Ying Han: Conceptualization, funding acquisition, and project administration. Shufang Li: Conceptualization, experiments, and writing – original draft. Mingxing Lu, Zijian Liu, Jianqiu Jin, and Qianyun Guo: Resources and inspect. Each author contributed to the preparation of the manuscript and agreed with the submission in its present form.

ACKNOWLEDGMENT

The present study was supported by the National Natural Science Foundation of China (Grant nos. 81771071, 81977920, and 81772873).

CONFLICTS OF INTEREST

The authors declare no conflicts of interest.

PEER REVIEW

The peer review history for this article is available at https://publons.com/publon/10.1111/jop.13321.

DATA AVAILABILITY STATEMENT

The data that support the findings of this study are available from the corresponding author upon reasonable request.

ORCID

Shufang Li https://orcid.org/0000-0002-3949-7849

REFERENCES

1. Siegel RL, Miller KD, Jemal A. Cancer statistics, 2019. *CA Cancer J Clin*. 2019;69(1):7-34.
2. Guo X, Han Y, Liu ZJ, Li SF, Huang GD, Liu HW. Expert recommendations for prevention, treatment and care of oral ulcers and other mucosal diseases during the coronavirus outbreak. *Chin J Dent Res*. 2020;23(2):95-98.
3. Panarese I, Aquino G, Ronchi A, et al. Oral and oropharyngeal squamous cell carcinoma: prognostic and predictive parameters in the etiopathogenetic route. *Expert Rev Anticancer Ther*. 2019;19(2):105-119.
4. Chaturvedi AK, Udaltsova N, Engels EA, et al. Oral leukoplakia and risk of progression to oral cancer: a population-based cohort study. *J Natl Cancer Inst*. 2020;112(10):1047-1054.
5. Ho PS, Wang WC, Huang YT, Yang YH. Finding an oral potentially malignant disorder in screening program is related to early diagnosis of oral cavity cancer – experience from real world evidence. *Oral Oncol*. 2019;89:107-114.
6. Peltanova B, Raudenska M, Masarik M. Effect of tumor microenvironment on pathogenesis of the head and neck squamous cell carcinoma: a systematic review. *Mol Cancer*. 2019;18(1):63.
7. Kämmerer PW, Al-Nawas B, Kalkan S, et al. Angiogenesis-related prognosis in patients with oral squamous cell carcinoma-role of the VEGF +936 C/T polymorphism. *J Oral Pathol Med*. 2015;44(6):429-436.
8. Pazouki S, Chisholm DM, Adi MM, et al. The association between tumour progression and vascularity in the oral mucosa. *J Pathol*. 1997;183(1):39-43.
9. Shen J, Zhu W. Research advances in the role of gastric cancer-derived mesenchymal stem cells in tumor progression (review). *Int J Mol Med*. 2021;47(2):455-462.
10. Atiya H, Frisbie L, Pressimone C, Coffman L. Mesenchymal stem cells in the tumor microenvironment. *Adv Exp Med Biol*. 2020;1234:31-42.
11. Melzer C, Yang Y, Hass R. Interaction of MSC with tumor cells. *Cell Commun Signal*. 2016;14(1):20.
12. Chen A, Wang H, Su Y, et al. Exosomes: biomarkers and therapeutic targets of diabetic vascular complications. *Front Endocrinol*. 2021;12:720466.
13. Wang L, Yin P, Wang J, et al. Delivery of mesenchymal stem cells-derived extracellular vesicles with enriched miR-185 inhibits progression of OPMD. *Artif Cells Nanomed Biotechnol*. 2019;47(1):2481-2491.
14. Fujiwara T, Eguchi T, Sogawa C, et al. Carcinogenic epithelial-mesenchymal transition initiated by oral cancer exosomes is inhibited by anti-EGFR antibody cetuximab. *Oral Oncol*. 2018;86:251-257.
15. Ji X, Zhang Z, Han Y, et al. Mesenchymal stem cells derived from normal gingival tissue inhibit the proliferation of oral cancer cells in vitro and in vivo. *Int J Oncol*. 2016;49(5):2011-2022.
16. Li WD, Zhou DM, Sun LL, et al. LncRNA WTAPP1 promotes migration and angiogenesis of endothelial progenitor cells via MMP1 through microRNA 3120 and Akt/PI3K/autophagy pathways. *Stem Cells*. 2018;36(12):1863-1874.
17. Li W, Han Y, Zhao Z, et al. Oral mucosal mesenchymal stem cell-derived exosomes: a potential therapeutic target in oral premalignant lesions. *Int J Oncol*. 2019;54(5):1567-1578.

18. Zhao W, Qin P, Zhang D, et al. Long non-coding RNA PVT1 encapsulated in bone marrow mesenchymal stem cell-derived exosomes promotes osteosarcoma growth and metastasis by stabilizing ERG and sponging miR-183-5p. *Aging*. 2019;11(21):9581-9596.
19. Thiem DGE, Schneider S, Venkatraman NT, et al. Semiquantifiable angiogenesis parameters in association with the malignant transformation of oral leukoplakia. *J Oral Pathol Med*. 2017;46(9):710-716.
20. Pittayapruek P, Meephansan J, Prapapan O, Komine M, Ohtsuki M. Role of matrix metalloproteinases in photoaging and photocarcinogenesis. *Int J Mol Sci*. 2016;17(6):868.
21. Gabasa M, Radisky ES, Ikemori R, et al. MMP1 drives tumor progression in large cell carcinoma of the lung through fibroblast senescence. *Cancer Lett*. 2021;507:1-12.
22. Yu CL, Yu YL, Yang SF, et al. Praeruptorin A reduces metastasis of human hepatocellular carcinoma cells by targeting ERK/MMP1 signaling pathway. *Environ Toxicol*. 2021;36(4):540-549.
23. Sutinen M, Kainulainen T, Hurskainen T, et al. Expression of matrix metalloproteinases (MMP-1 and -2) and their inhibitors (TIMP-1, -2 and -3) in oral lichen planus, dysplasia, squamous cell carcinoma and lymph node metastasis. *Br J Cancer*. 1998;77(12):2239-2245.
24. George A, Ranganathan K, Rao UK. Expression of MMP-1 in histopathological different grades of oral squamous cell carcinoma and in normal buccal mucosa – an immunohistochemical study. *Cancer Biomark*. 2010;7(6):275-283.
25. Sapkota D, Bruland O, Costea DE, Haugen H, Vasstrand EN, Ibrahim SO. S100A14 regulates the invasive potential of oral squamous cell carcinoma derived cell-lines in vitro by modulating expression of matrix metalloproteinases, MMP1 and MMP9. *Eur J Cancer*. 2011;47(4):600-610.
26. Wu C, Yu J, Xu G, et al. Bioinformatic analysis of the proteome in exosomes derived from plasma: exosomes involved in cholesterol metabolism process of patients with spinal cord injury in the acute phase. *Front Neuroinform*. 2021;15:662967.

SUPPORTING INFORMATION

Additional supporting information may be found in the online version of the article at the publisher's website.

How to cite this article: Li S, Han Y, Lu M, et al. Mesenchymal stem cell-exosome-mediated matrix metalloproteinase 1 participates in oral leukoplakia and carcinogenesis by inducing angiogenesis. *J Oral Pathol Med*. 2022;51(7):638-648. doi:10.1111/jop.13321